Resilience Assessment and Improvement for Cyber-Physical Power Systems Under Typhoon Disasters

Baozhong Ti, Gengyin Li, *Member, IEEE*, Ming Zhou, *Senior Member, IEEE*, and Jianxiao Wang, *Member, IEEE*

***Abstract*—The cyber-physical deep coupling makes power systems face more risks under small-probability and high-risk typhoon disasters. Resilience describes the ability of cyber-physical power system (CPPS) withstanding extreme disasters and resuming normal operation. To improve the resilience assessment and analysis method of CPPS, first, a CPPS resilience assessment framework that considers the space-time metrics of disasters and the interactions of information systems and power grids is proposed, including fault scenarios extraction, response and recovery analysis, quantitative assessment of resilience. Second, from the perspective of the geographical coupling between OPGW and transmission lines and the control coupling between automatic generation control system (AGC), substation automation system (SAS) and power system, the interaction of information flow and energy flow during the failure period is analyzed. The network flow theory is used to establish an information network traffic model to describe the operating status of the information system at each stage. On this basis, a mixed integer linear programming model for DC optimal power flow considering the information network constraints and a multi-stage bi-level model for cyber-physical collaborative recovery are established. Finally, we take the IEEERTS-79 system as an example to show that the proposed method can improve the quantization accuracy comparing with the assessment method of the conventional power system, and evaluate the enhancement of typical measures at different stages.**

***Index Terms*—Resilience assessment, cyber-physical power system, typhoon disasters, information network traffic model, collaborative recovery.**

I. Introduction

EXTREME weather disasters occur more frequently with global comate change, which poses a great threat to power system operation and brings vast economic losses [1], [2]. While the development and integration of information technology has improved the automation level of power systems, it has also brought challenges to its safe operation [3]. For example, in 2003, power outage occurred in the United States and Canada because the software failure of the information system affected the operation mode and controllability of the power system [4]. In 2008, due to ice and snow disasters in many southern provinces of China, the cyber-physical layer in the region failed at the same time, causing large-scale failures [5]. Therefore, it is necessary to study the resilience of the power system in the cyber-physical coupling environment and the corresponding improvement measures to reduce the impact of meteorological disasters.

Resilience, which is derived from materials science, refers to the ability of a material to return to its original shape after deformation. The resilience of the power system mainly refers to the ability to maintain and restore normal functions in the face of serious accidents, extreme disasters or attacks [6]. The resilience triangle model [7] and trapezoidal model [8] theories have been applied to the construction of indicators. An improved resilience indicator was proposed considering the characteristics of extreme events in [9]. In [10], a planning-oriented resilience assessment framework was proposed to quantify the transmission system resilience from the perspectives of the component and identify its weak points. The related improvement measures mainly include disaster defenses and post disaster recovery. Reference [11] selected the optimum reinforcement location that is most conducive to improving the resilience of the distribution network and provided strengthening strategies through a three-stage optimization model. A defensive islanding algorithm was proposed to mitigate the cascading effects that may occur during weather emergencies in [12]. Studies on post disaster recovery have also penetrated deeply. From the initial emergent plan formulation and expert system assistance to reconfiguration and load recovery [13]–[15], there are an increasing number of ways to improve recovery efficiency.

Compared with the abundant research basis of power system resilience, there are few studies on resilience assessment of cyber-physical power system (CPPS). Reference [16] proposed a resilience measurement method from the perspective of the intrusion tolerance mechanism and the recovery capability, and use Markov information defense strategies to improve resilience under cyber attacks. In [17], physical resiliency metric was provided based on a mix of infrastructure and operational indices. Cyber resiliency metric was quantified ability of communication and the security mechanisms.

Manuscript received April 14, 2021; revised August 2, 2021; accepted September 14, 2021. Date of publication September 22, 2021; date of current version December 23, 2021. This work was supported by the National Key Research and Development Program of China under Grant 2016YFB0901100. Paper no. TSG-00564-2021. *(Corresponding author: Gengyin Li.)*

The authors are with the State Key Laboratory of Alternate Electrical Power System with Renewable Energy Sources, North China Electric Power University, Beijing 102206, China (e-mail: tibaozhong@163.com; ligy@ncepu.edu.cn; zhouming@ncepu.edu.cn; wangjx@ncepu.edu.cn).

Color versions of one or more figures in this article are available at https://doi.org/10.1109/TSG.2021.3114512.

Digital Object Identifier 10.1109/TSG.2021.3114512

On that basis, a cyber-physical resiliency assessment metric for the transmission electric grid is proposed. By using concepts from graph theoretic analysis, probabilistic model of availability, quantitative factors affecting microgrid, system resiliency was identified and a cyber-physical security assessment metric was proposed through a multi-criteria decision making (MCDM) technique in [18]. Resilience improvement of CPPS is of great significance for reliability enhancement of power supply and risk reduction for propagation of faults across space in the face of multiple cyber-physical uncertainties. From the perspective of information systems, considering the risk of communication transmission in EMS, a dynamic optimization mechanism for alternate communication routes is proposed in [19]. Reference [20] proposed a robust optimization strategy for communication routing that considers the cyber-physical disturbances. From the perspective of the physical power grid, [21] described information system operation by establishing the state indicator of the communication link between controlled node and control center, and proposed an optimal power flow model constrained by information networks. Reference [22] established a network topology optimization method to mitigate the coordinated cyber-physical attacks. However, the present improvement methods mostly focus on disaster resistance. The enhancement measures at different stages such as predictive protection and post disaster recovery also play an important role on system's ability to cope with extreme disasters.

In conclusion, the research on CPPS resilience assessment is still at the initial stages. The system not only have the interdependence of the control systems and power supply, but also have geographic coupling. For example, the optical fiber is often put in the ground wire of the overhead high-voltage transmission line to form the optical fiber composite overhead ground wire (OPGW) [20]. The topology of these communication networks is consistent with that of the power grid. This multi-coupling feature causes that the intensity and location of meteorological disasters can affect the transmission of information flow and energy flow differently. Some extreme scenarios may lead to cyber-physical coupling failures, which increases the state space and complicates evaluation process. At the same time, most of the existing improvement methods focus on withstanding extreme scenarios. The power system with high intelligent level also has the resilience enhancement potential in other fault stages. The application of technologies such as accident warning and fault location will effectively improve the response capability of the system. Online recovery technology, dispatch automation and substation automation improve the system's ability to deal with emergencies and reduce maintenance time [23]. Therefore, it is of great practical significance to study the coupling effect of the information system and the power system during the fault period, reduce its negative impact on power fault propagation, and develop its superiority regarding system intelligence.

Under this background, we propose a CPPS resilience assessment method considering space-time characteristics of disasters and cyber-physical multi-coupling features. To describe the operating status of the information system at different stages quantitatively, similar to the power flow model, an information network traffic model is established based on network flow theory, which serves as a constraint condition for the operation of the information system in the failure phase and recovery phase. Since most studies focused on improvements at fault response stage, from the perspective of the actual control system and the coupling interface, this paper analyzes the interactions between the information system and the power system in the response phase and the recovery phase, and establishes an information-physical coupling model. On this basis, an optimal power flow (OPF) model considering the information network constraints and a multi-stage bi-level model for cyber-physical collaborative recovery are established respectively. Combined with the proposed assessment framework, CPPS resilience is assessed considering fault stages and disaster scenarios comprehensively.

The remainder of this article is organized as follows. Section II analyzes cyber-physical interdependence in CPPS and establishes evaluation framework. Section III studies the impact of typhoon weather on component failure rates, analyzes the cyber-physical coupling effect during the failure period and proposes the information network traffic model. In Section IV, the CPPS response model and recovery model are established. Section V verifies the effectiveness of the method through case study, and Section VI gives the conclusion.

II. Resilience Assessment of CPPS

A. Cyber-Physical Interdependence Analysis

A CPPS includes a physical power system and information system. The physical power system mainly includes electrical primary equipment, which is responsible for the reliable operation of the power generation, transmission, distribution, and utilization, as well as power supply for communication equipment. The information system includes a control center, communication network and intelligent interfaces composed of automatic generation control (AGC), remote terminal units (RTU), automatic voltage control (AVC), phasor measurement units (PMU), distribution transformer supervisory terminal units (TTU), data transfer units (DTU), etc., which are mainly responsible for information collection, monitoring and decision control of the entire system.

The dispatching automation system adopted by the control center includes supervisory control and data acquisition (SCADA), energy management system (EMS) and management information systems (MIS), which are responsible for data acquisition and processing, energy management and network analysis, and information maintenance to ensure the safe operation of the power grid. The coupling relationship between information equipment and power equipment is shown in Fig. 1.

According to complex network theory, the physical power system is represented by $G_P = (V_P, E_P)$, where V_P is the power node set and represents power system bus with functional attributes including power generation, substation and load. E_P is the power line set which represents power transmission lines. The information system is represented by $G_C = (V_C, E_C)$, where V_C is the information node set and represents control center and communication terminal with

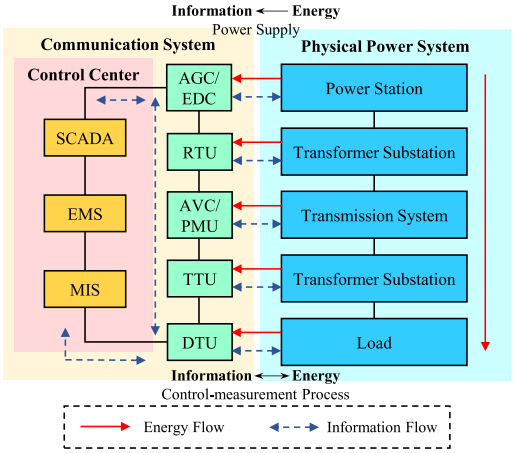

Fig. 1. Typical structure of cyber-physical power system.

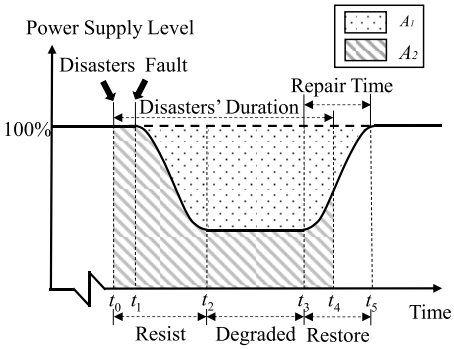

Fig. 2. The function curve of the power system under extreme natural disasters.

different functions such as dispatching, relaying and monitoring in the network. E_C is the information line set which represents the communication channel between information network sites.

B. Assessment Model

When extreme typhoon disasters occur, if the system's resistance is insufficient, a large number of power and communication components may fail which will lead to a large-scale power outage and power communication interruption. When the system performance degrades, it is restored to its normal state through various response and repair measures. The missing area of load curve is adopted to reflect the CPPS resilience, which is shown in Fig. 2.

The missing area reflects the extent of damage during the disaster. In this paper, the power-supply level is used as an indicator to measure the system function. According to the model in [9], the area $[t_0, t_1]$ should be considered in the evaluation considering that short-term disasters may not affect the operation of high resilience system.

The conventional method [8] does not distinguish the intervals at different stages, and long-term maintenance of minor faults will increase system resilience assessments. Reference [9] proposes a new resilience index based on the above method, considering the duration of different stages and introducing a time coefficient in the evaluation. However, the evaluation result will be too small at long maintenance

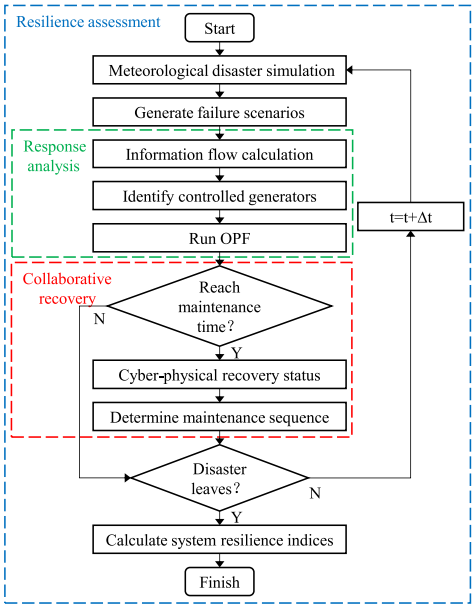

Fig. 3. The resilience assessment steps.

time. Actually, the larger the area of the normal-fault curve in $[t_4, t_5]$ encircles, the lower the resilience level of the system should be.

We draw on the area partition idea of the above index, and the area that the normal-fault curve in $[t_4, t_5]$ encircles is removed from the numerator to the denominator. Then the situations can be distinguished. Combining the failure scenario rate, resilience evaluation indicators R_{EI} are established as follows:

$$\begin{aligned} R_{EI} &= E\left(\int_{t_0}^{t_4} R_{Pdisaster}dt \Big/ \left(\int_{t_0}^{t_4} R_{Pnormal}dt \right.\right. \\ &\quad \left.\left. + \int_{t_4}^{t_5} (R_{Pnormal} - R_{Pdisaster})dt\right)\right) \\ &= \sum_{s \in S_{disaster}} p_s \frac{A_2}{A_1 + A_2} \end{aligned} \tag{1}$$

where $E(\cdot)$ represents the expected value. p_s represents the incidence of fault scenario s. $S_{disaster}$ is the scenario set, and $R_{Pnormal}$ and $R_{Pdisaster}$ are the normal operating function curve and fault operating function curve respectively. A_1 is the missing area of the function curve. A_2 is the area of fault curve during the resist and degraded period.

Different from the conventional power system resilience assessment, the evaluation of CPPS needs to consider cyber-physical coupling in all evaluating process. The resilience assessment process of the CPPS under extreme typhoon disasters is shown in Fig. 3. The failure rate model of power components and communication components is proposed in Section III. A detailed introduction to the response analysis and collaborative recovery is given in Section IV. Before the simulation, the circuit is divided into several units to calculate the wind speed and fault probability. Random numbers with uniform distribution among [0, 1] are generated and sampled by the Monte Carlo method to determine the operating state of the components. The evaluation index is calculated according to the overall operating state at each step.

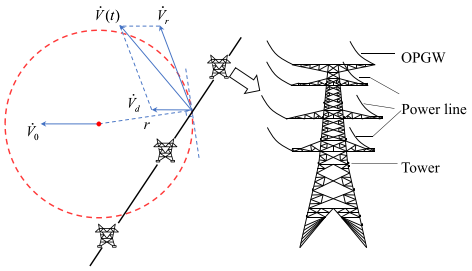

Fig. 4. The position relation between typhoon and transmission corridors.

III. Influence of Typhoon Disasters on CPPS

A. The Component Failure Model Under Extreme Weather Conditions

The impact of extreme weather on CPPS varies with time and geography. Transformers and cables in the transmission system are almost immune to strong breezes [24]. Overhead lines and towers are more likely to be damaged by typhoons, so we focus on the faults of lines and towers only.

At present, communication optical fibers are often placed in the bottom line of overhead high-voltage transmission lines to form the OPGW. Therefore, the transmission grid topology and its communication network are highly coupled [20], and easily affected by extreme weather. This paper uses the same overhead line fault model when calculating the failure rate of the two types. The structure of the overhead line and the positional relationship between the typhoon and the transmission corridor are shown in Fig. 4.

The instantaneous wind speed $V(t)$ in the typhoon wind field is summarized by the moving wind speed V_d and the circulating wind speed V_r. The Miyazaki model is used to calculate V_d [25]. Assuming that the typhoon has circular symmetry, we use the Rankine model to calculate V_r [26].

$$V_d = V_0 e^{-\pi r/10R_{\max}} \tag{2}$$

$$V_r = \begin{cases} \frac{r}{R_{\max}} V_{r\max} & 0 \le r \le R_{\max} \\ \frac{R_{\max}}{r} V_{r\max} & r > R_{\max} \end{cases} \tag{3}$$

in which

$$r = 6371 \arccos(\sin y_1 \sin y_2 + \cos y_1 \cos y_2 \cos(x_1 - x_2)) \tag{4}$$

$$V_{r\max} = V_{\max} - V_0 e^{-\pi/10} \tag{5}$$

$$V_0 e^{-\pi r/10R_{\max}} + \frac{R_{\max}}{r_7} V_{r\max} = V_{7\min} \tag{6}$$

where V_0 is the travel speed of the typhoon center. The circulating wind speed V_r has an inner deflection angle along the tangent direction which is approximately 20°. Here, r is the distance from a certain point in the wind field to the typhoon center which can be obtained from the latitude and longitude coordinates (x_1, y_1) and (x_2, y_2). $V_{r\max}$ and $V_{\max}$ are the maximum circulating wind speed and the wind speed near the center, respectively. $R_{\max}$ is the maximum wind speed radius, and r_7 is the radius of the 7-level wind whose low limit value $V_{7\min}$ is 13.9 m/s.

The instantaneous failure rates of the conductor and the tower are expressed as [10], [27],

$$\lambda_{wire,i}(t) = \sum_{j \in W_i} \exp\left(a \frac{v_i(t)}{V_{d,wire}} + b\right) \Delta L_i / 50 \tag{7}$$

$$\lambda_{tower,i}(t) = \begin{cases} 0 & v(t) \le V_{d,tower} \\ \exp(c(v(t) & V_{d,tower} \le v(t) \le 2V_{d,tower} \\ \quad -2V_{d,tower})) & \\ 1 & v(t) \ge 2V_{d,tower} \end{cases} \tag{8}$$

where $\lambda_{wire,l}(t)$ is the instantaneous failure rate of unit length conductor i at time t, which is characterized by the number of conductor failures per hour and per 50 km. $v_i(t)$ is the effective wind speed of section i in the line at time t. $V_{d,wire}$ and $V_{d,tower}$ are the design wind speeds of the conductor and the tower, respectively; and a and b are obtained from the historical statistical data of lines. W_l is the segment set of line l.

The line failure rate $p_{wire,l}$ and the tower failure rate $p_{tower,i}$ in the time period $[t_0, t_0 + \Delta t]$ can be expressed as [10],

$$p_{wire,l}(t_0, t_0 + \Delta\ t) = 1 - \exp\left(-\int_{t_0}^{t_0+\Delta t} \lambda_{wire,l}(t) dt\right) \tag{9}$$

$$p_{tower,i}(t_0, t_0 + \Delta t) = 1 - \exp\left(-\int_{t_0}^{t_0+\Delta t} \frac{\lambda_{tower,i}(t)}{1 - \lambda_{tower,i}(t)} dt\right) \tag{10}$$

Both the faults of conductors and towers can affect the normal operation of overhead lines. Therefore, the overhead line fault model $p_{line,l}$ is equivalent to a series system composed of conductors and towers, which can be expressed as follows:

$$p_{line,l} = 1 - \prod_{i \in L_{T,l}} (1 - p_{tower,i}) \prod_{i \in L_{W,l}} (1 - p_{wire,i}) \tag{11}$$

B. The Impact of the Power System on the Information System

The normal operation of the information node requires the power supply from the power node. It is worth pointing out that information nodes are generally equipped with uninterruptible power supply (UPS) which ensures the electricity supply in a short time. However, in practice, some UPSs can provide power within hours [28] and there are situations in which information nodes do not get sufficient power and cannot work normally [21]. In order to study the influence of the cyber-physical interaction on fault propagation, this paper runs the worst-case simulation. We assume that except for the control center and the information nodes corresponding to the no-load power node, the rest nodes are not equipped with UPS. This power-supply relationship can be expressed by coupling factor defined in [28],

$$Z_{i'} = \begin{cases} 1 & P_{Di} \ge \alpha P_{Di,0} \\ 0 & P_{Di} < \alpha P_{Di,0} \end{cases} \qquad i \in V_E, i' \in V_C \tag{12}$$

where $Z_{i'}$ denotes the power supply status of information node i'. The factor is 1 if the power supply status is normal. P_{Di} and $P_{Di,0}$ are the current load and initial load of node i respectively, and α $(0 \le \alpha \le 1)$ is the power-supply

coefficient reflecting the coupling strength between the two networks. The larger the value α takes, the greater the dependence on the power system the information system has and the more vulnerable the information networks are.

C. The Impact of the Information System on the Power System During Fault Phases

As the circuit breaker will disconnect the branch in time once the line is overloaded, this typical switch can act without commands from the control center [29]. Therefore, we take the generator as the cyber-physical interaction point. In a highly integrated environment, the normal operation of generating equipment requires monitoring and control from coupled information facilities. The control center calculates the control command based on the real-time operating status of the system which includes the frequency, generating power and interchange power of tie-lines. Then, the commands are transmitted to the generator through the communication channel, SCADA and RTU [30]. When a power failure causes large disturbances, if the generator control equipment fails, the AGC system in the EMS has not been triggered to adjust the generator output. Unbalanced power occurs in the system, causing destabilizing oscillation, voltage and frequency fluctuations, which triggers frequency protection that leads to generator tripping [31]. This relationship can be described as

$$\phi_{i'} P_{Gi}^{\min} \le P_{Gi} \le \phi_{i'} P_{Gi}^{\max} \qquad i \in V_{PG}, i' \in V_C \tag{13}$$

where $\phi_{i'} \in \{0, 1\}$ is the working status of information node i' corresponding to power generation node i. If the node works normally, $\phi_{i'} = 1$. P_{Gi}, P_{Gi}^{min} and P_{Gi}^{max} are the generated power, and minimum and maximum output limits of node g respectively. V_{PG} is the generation node set.

D. The Impact of the Information System on the Power System During Recovery Phases

The information system failure will deactivate the AGC and block the generator from receiving power adjustment commands from the control center. At this moment, it is necessary to keep contact with the control center through telephone and mail communication which are generally equipped with backup power and complete monitoring systems [32], and adjust outputs manually resulting in a slower response and extended recovery time. The influence of information failure on generator recovery is shown in Fig. 5 (a), which will result in a smaller adjustment range for generated power. In other words, the uncontrollability of the generator at previous stage will lead to its output range reduction at this stage, which can be described as

$$P_{Gi,t}^{\max} = \begin{cases} 0 & 0 \le t < t_{start} + \Delta T_{Gi}\left(1 - \phi_{i',t-1}\right) \\ P_{Gi}^{\min} + K_g(t - t_{start}) & t_{start} + \Delta T_{Gi}\left(1 - \phi_{i',t-1}\right) \le t < t_{end} \\ P_{Gi}^{\max} & t \ge t_{end} \end{cases} \tag{14}$$

where $P_{Gi,t}^{max}$ is the maximum available power of generator node g at time t. K_g and ΔT_{Gi} are the ramp rate and the manual adjustment time for the generator, and t_{start} and t_{end} are the initial time and the end time of adjustment respectively. $P_{g,supply}$ in Fig. 5 (a) is the generating auxiliary power. This paper assumes that the generators in the case study have the function of fast load shedding, and they can operate stably with auxiliary power after being separated from the network.

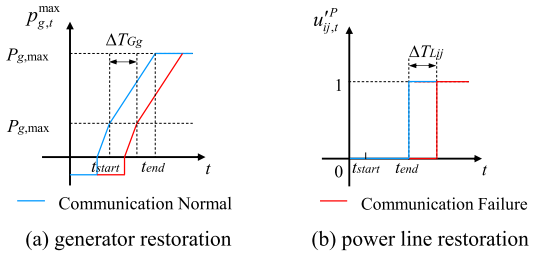

Fig. 5. The impact of information failure on generator output and power lines restoration.

With the technology of dispatch automation and substation automation gradually maturing, equipment such as circuit breakers can be controlled remotely [33], which helps the power system to handle emergencies quickly. Information system failures will also lead to substation automation system (SAS) failure. Power equipment such as circuit breakers, isolating switches and load switches requires manual operation. Compared with the automated operation of SAS, the manual operation requires a series of processes from filling the operation ticket to the final execution, which requires additional time. The influence of information failure on the transmission line recovery is shown in Fig. 5 (b). If the control function at one end of line failed at previous stage, this line will take more time to recover at this stage. Here we assume that the additional required time at both ends is equal. The influence can be described as

$$u_{ij,t}^{'P} = \begin{cases} 0 & 0 \le t < t_{start} + \Delta T_{Lij} \cdot \left(2 - \phi_{i',t-1} - \phi_{j',t-1}\right)/2 \\ 1 & t \ge t_{start} + \Delta T_{Lij} \cdot \left(2 - \phi_{i',t-1} - \phi_{j',t-1}\right)/2 \end{cases} \tag{15}$$

where $u'^{P}_{ij,t}$ is the operating state of the line at time t in the recovery phase. ΔT_{Lij} is the additional time required for manual recovery.

E. Information Network Traffic Model

The operation of the information network does not need to satisfy Kirchhoff's law like the power network. In general, the normal operation of the information node depends on the following two points: 1) there is a transmission path connected to the control center and; 2) the node receives enough power supply. Therefore, the working status of the information node is determined by the power supply status from the corresponding power node and the operating status of the communication link to the control center.

The above problem can be explained by network flow theory. We represent the information flow as a single-source and multi-sinks network, as shown in Fig. 6. The information nodes and links are the vertices and arcs of the graph, and the information flow and its bandwidth are the network traffic and capacity respectively.

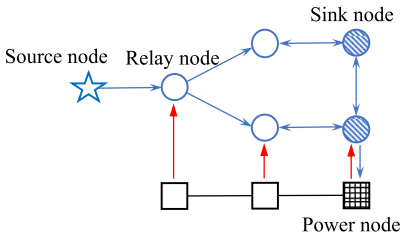

Fig. 6. Single-source multi-sinks network of information flow.

The source node is the control center. The relay node is the information node that the information flow passes through. The sink node is the information node whose status needs to be determined, such as generation nodes and info nodes coupled with failure lines in the recovery phase. When the flow from the source to the sink meets the following two constraints: 1) the flow on each arc is less than the rated capacity and; 2) the inflow of the relay node is equal to the outflow, this flow can be called as a network feasible flow.

The working status of the information node is a decision variable, which is a Boolean number and is taken as 1 when there is a feasible flow between this node and the control center.

$$\phi_k \in \{0, 1\} \qquad k \in V_{C.sink} \tag{16}$$

where: ϕ_k is the working status for node k. $V_{C,sink}$ is the destination node set which is composed of the controlled node.

The source node, as the sender of the information flow, has only outgoing traffic but no incoming traffic, so the communication traffic on the link connected to it satisfies

$$\begin{cases} \sum\limits_{k\in V_{C.sink}} \sum\limits_{j':(i',j')\in E_C} I^k_{i'j'} \le \phi_k B_k \\ \sum\limits_{j':(i',j')\in E_C} I_{j'i',k} = 0 \end{cases} \qquad i' \in V_{C.src} \tag{17}$$

where: $I_{i'j',k} \in \{0, 1\}$ is the decision variable of communication follow about control node k on link (i', j') . B_k is the required bandwidth. $V_{C,src}$ is the source node set, that is, the control center node.

The relay node mainly plays the role of service transmission. The incoming flow and outgoing flow through the node should be equal. In addition to transmitting services, the sink node also executes instructions from the control center and consumes communication traffic. So its incoming traffic should include outgoing traffic and the traffic required by terminal equipment.

Traffic transmission on these nodes is expressed by equation (18) uniformly. For the relay node, $\phi_k = 0$.

$$\sum_{k\in V_{C.sink}} \sum_{j':(i',j')\in E_C} I^k_{j'i'} = \sum_{k\in V_{C.sink}} \sum_{j':(i',j')\in E_C} I^k_{i'j'} + \phi_k B_k \quad i' \in \bar{V}_{C.src} \tag{18}$$

The information node failure will disable the normal function of the link connected to it. The communication traffic on the information link (i', j') should not only exceed the bandwidth $B^{max}_{i'j'}$, but also be constrained by the power-supply state $Z_{i'}$. This relationship is modeled as follows:

$$0 \le \sum_{k\in V_{C.sink}} I^k_{i'j'} B_k \le \min\left\{Z_{i'} \cdot B^{\max}_{i'j'}, Z_j \cdot B^{\max}_{i'j'}\right\} \tag{19}$$

The service transmission should not exceed the allowable time delay. Some communication services such as line protection services and load frequency control (LFC) have strict delay requirements [34], [35]. The communication delay is determined by the transmission delay of the selected link.

$$0 \le \sum_{(i',j')\in E_C} I^k_{i'j'} T_{i'j'} \le T^{\max}_k \qquad k \in V_{C.sink} \tag{20}$$

where $T_{i'j'}$ is the transmission delay of the link (i', j'), and B^{max}_k is the allowable delay of the service on node k.

By linearizing the network flow model, the above can be taken as a mixed integer constraint of OPF and solved rapidly by commercial software.

IV. System Response and Recovery

A. The Response Models

When the extreme disaster causes the overhead line failure, the control function may fail due to insufficient energy supply, which may lead to cascading failures between the physical power grid and the information system.

We assume that power lines can also run in overload within the hot limit in emergency dispatching period [36]. The number of fault stages is defined as h and the system's response is to minimize the loss of load at each stage as the goal. The DC power flow model has the merits of less parameters and fast convergence speed, which is widely used in CPPS risk assessment [21], [22]. By introducing control functions and information flow transmission constraints, the mixed integer linear programming model of OPF is established, as shown in equations (21)-(26).

The input variables are the communication link state $e^C_{i'j',h}$ and the transmission line state $e^P_{ij,h}$. When typhoons interrupt the communication link or the power line, the variable value is 0. The optimized variable is the generator output $\boldsymbol{P}_{G,h}$.

$$\min \sum_{i\in V_P} \left(P_{Di,0} - P_{Di,h}\right)$$

$$\text{s.t.} \quad (12), (13), (16) - (18), (20) \tag{21}$$

$$0 \le \sum_{k\in V_{C.dest}} I^k_{i'j',h} B_k \le \min\Big\{Z_{i',h} \cdot B^{\max}_{i'j'} \cdot e^C_{i'j',h}, Z_{j',h} \cdot B^{\max}_{i'j'} \cdot e^C_{i'j',h}\Big\} \qquad i', j' \in V_C \tag{22}$$

$$\mathbf{A}_{NL}\mathbf{F}_h = \mathbf{A}_{NG}\mathbf{P}_{G,h} + \mathrm{A}_{ND}\mathbf{P}_{D,h} \tag{23}$$

$$F_{ij.h} = e^P_{ij,h} b_{ij} \sum_{i\in V_P} a^T_{NL,(i,j)} \theta_{i,h} \qquad (i,j) \in E_P \tag{24}$$

$$0 \le P_{Di,h} \le P_{Di,0} \qquad i \in V_P \tag{25}$$

$$-F^{\max}_{ij} e^P_{ij,h} \le F_{ij,k} \le F^{\max}_{ij} e^P_{ij,h} \qquad (i,j) \in E_P \tag{26}$$

where $P_{Di,0}$ and $P_{Di,h}$ are the load power and the reduced load of node i in period h. $\boldsymbol{A}_{NL}$, $\boldsymbol{A}_{NG}$ and $\boldsymbol{A}_{ND}$ are the node-branch, power node-generation node and power node-load node incidence matrix respectively. $a^T_{NL,(i,l)} \epsilon \boldsymbol{A}^T_{NL}$. $\boldsymbol{F}_h$, $\boldsymbol{P}_{G,h}$ and $\boldsymbol{P}_{D,h}$ are the power flow matrix, generating power matrix and load

power matrix in period m respectively. $F_{ij,h}$ and $F_{ij}^{\max}$ are the power flow and the transmission capacity of line (i, j). b_{ij} is the element of nodal admittance matrix corresponding to (i, j). $\theta_{i,h}$ is the power angle of node i.

Equations (12) and (13) are the operation constraints for the information node and generator output. Equations (16)-(18) and (20) simulates the transmission process of the information service from the control center to the intelligent terminal at stage h. The input variable $e_{i'j',h}^{C}$ of the information system acts on equation (22), which is the bandwidth constraint. Equations (23), (24) represent the power balance constraint. The equations (25) and (26) show the constraints of the load reduction and branch flow.

B. The Recovery Models

The information system provides more flexible methods for the operation and restoration of the power system. Using the monitoring function, the maintenance efficiency of fault lines after a disaster can be improved. Moreover, the information equipment will also be affected by natural disasters, resulting in the unavailability of information functions. To solve this problem, considering the interaction between the two systems, a collaborative recovery strategy is formulated. The input variables are scenarios failure sets $E'_C = \{e_{i'j',m}^{C} = 0\}$ and $E'_P = \{e_{ij,m}^{P} = 0\}$. The optimized variables are the initial maintenance period of the communication line $t_{i'j'}^{C}$ and the initial maintenance period of the transmission line t_{ij}^{P}.

The system repair aims at the smallest decline area of the function curve during the entire restoration phase. A bi-level programming model is adopted to describe the collaborative recovery of communication networks and power grids. The upper model represents the maintenance scheduling and the communication network operation, and establishes the objective function with the goal of the fastest recovery of the system's function curve. The lower model builds the OPF based on the repair schedule constraints, and establishes the objective function with the minimum load reduction in each recovery stage. The upper model passes the fault line state $e_{ij,m}^{P}$ and the generator control status $\phi_{i',m}$ at maintenance phase m to the lower model. the lower model uploads the load matrix $\boldsymbol{P}_{D,m}$ to update the power supply status $Z_{i',m}$ for the information node. The collaborative recovery model is as follows:

$$\min \quad \sum_{m}\sum_{i\in V_P}\left(P_{Di,0}-P_{Di,m}\right)\Delta t_m$$

$$\text{s.t.} \quad (12),\ (16)-(18),\ (20),\ (22) \tag{27}$$

$$\sum_{m\Delta\ t_m=t_{i'j'}^{C}}^{N_{rec}} h_{i'j',m}^{C}\Delta t_m = T_{i'j'}^{CL} \qquad \left(i',j'\right)\in E'_C \tag{28}$$

$$\sum_{(i',j')\in\mathbf{E}_C} h_{i'j',m}^{C} \le R_{PC} \tag{29}$$

$$e_{i'j',m}^{C}=\begin{cases}1 & m\Delta t_m \ge t_{i'j'}^{C}+T_{i'j'}^{CL}\\ 0 & m\Delta t_m < t_{i'j'}^{C}+T_{i'j'}^{CL}\end{cases} \qquad \left(i',j'\right)\in E'_C \tag{30}$$

$$\sum_{m\Delta\ t_m=t_{ij}^{P}}^{N_{rec}} h_{ij,m}^{P}\Delta t_m = T_{ij}^{PL}+\Delta T_{L,ij}\cdot\left(2-\phi_{i',m-1}-\phi_{j',m-1}\right)/2$$
$$(i,j)\in E'_P \tag{31}$$

$$\sum_{(i,j)\in E_P} h_{ij,m}^{P} \le R_{PL} \tag{32}$$

$$e_{ij,m}^{P}=\begin{cases}1 & m\Delta t_m \ge t_{ij}^{P}+T_{ij}^{PL}+\Delta T_{L,ij}\cdot\left(2-\phi_{i',m-1}-\phi_{j',m-1}\right)/2\\ 0 & m\Delta t_m < t_{ij}^{P}+T_{ij}^{PL}+\Delta T_{L,ij}\cdot\left(2-\phi_{i',m-1}-\phi_{j',m-1}\right)/2\end{cases}$$
$$(i,j)\in E'_P, i', j'\in V_C \tag{33}$$

$$e_{i,m}^{G}=\begin{cases}1 & \sum\limits_{(g,i)\in\mathbf{E}_P} e_{ij,m}^{P}\ge 1\\ 0 & \sum\limits_{(g,i)\in\mathbf{E}_P} e_{ij,m}^{P}< 1\end{cases} \qquad i\in V'_{PG}, j\in V_P \tag{34}$$

$$\left(\mathbf{P}_{D,m}\right)=\arg\left\{\min\sum_{i\in V_P}\left(P_{Di,0}-P_{Di,m}\right)\right\}$$

$$\text{s.t.} \quad (25) \tag{35}$$

$$\mathbf{A}_{NL}\mathbf{F}_m=\mathbf{A}_{NG}\mathbf{P}_{G,m}+\mathrm{A}_{ND}\mathbf{P}_{D,m} \tag{36}$$

$$F_{ij.m}=e_{ij,m}^{P}b_{ij}\sum_{i\in V_P}a_{NL,(i,j)}^{T}\theta_{i,m} \qquad (i,j)\in E_P \tag{37}$$

$$P_{Gi,m}\ge\max\Big\{P_{Gi,m-1}+\left(e_{i,m}^{G}-e_{i,m-1}^{G}\right)\left(P_{Gi,\min}-K_{Gi}\Delta T_{G,i}\left(1-\phi_{i',m-1}\right)\right),e_{i,m}^{G}P_{Gi,\min}\Big\} \quad i\in V_{PG} \tag{38}$$

$$P_{Gi,m}\le\min\Big\{P_{Gi,m-1}+K_{Gi}\Delta\ t_m+\left(e_{i,m}^{G}-e_{i,m-1}^{G}\right)\left(P_{Gi,\min}-K_{Gi}\Delta T_{G,i}\left(1-\phi_{i',m-1}\right)\right),e_{i,m}^{G}P_{Gi,\max}\Big\} \quad i\in V_{PG} \tag{39}$$

$$-F_{ij}^{\max}e_{ij,m}^{P}\le F_{ij,m}\le F_{ij}^{\max}e_{ij,m}^{P} \quad (i,j)\in E_P \tag{40}$$

where Δt_m and N_{rec} are the duration of phase m and the total number of recovery phases. $h_{i'j',m}^{C}$ and $h_{ij,m}^{P}$ are the maintenance state variable of communication link (i', j') and power line (i, j) in period m, and the line or link is being repaired if the value is 1. $T_{i'j'}^{CL}$ and T_{ij}^{PL} are the required time of the link (i', j') repair and the line (i, j) repair respectively. E'_C, E'_P and V'_{PG} are the maintenance set of the link, the line and the generator. R_{PC} and R_{PL} are the maintenance resources for the link and the line. $\Delta T_{L,ij}$ and $\Delta T_{G,i}$ are the additional repair time of the line and the generator. $e_{i'j',m}^{C}$, $e_{ij,m}^{P}$ and $e_{i,m}^{G}$ are the recovery status of the link, the line and the generator.

Equations (12), (16)-(18), (20), (22) simulate the information system operation in phase m. Equation (28) represents the constrains of maintenance state variables of communication lines. Equation (29) indicates that the number of restored lines in each period cannot exceed the communication line maintenance resources such as maintenance teams. Equation (30) denotes the time limit of communication line repair. Different from the relative independence of each stage in the response process, there are progressive relationships in the recovery process. The recovery speed of lines and generators at stage m is determined by the control state at stage m-1. Equation (31) means that extra time is needed for artificial restoration of the line. Equation (32) indicates that the number of restored lines in the same period does not exceed the number of power line maintenance resources such as line maintenance teams. Equation (33) indicates that the line resumes normal operation after sufficient maintenance time. Equation (34) is the generator start-up constraint. Equations (38) and (39) means that the generator output range is affected by the coupled information node. Equations (36), (37), (40) are the constrains of power transmission.

Considering the complexity of the bi-level programming problem, we first linearize the nonlinear constraints, and then use the Lagrange multiplier algorithm to convert the lower

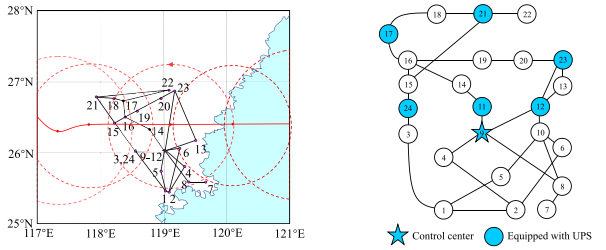

(a) geographical location (b)communication network

Fig. 7. IEEERTS-79 system structure.

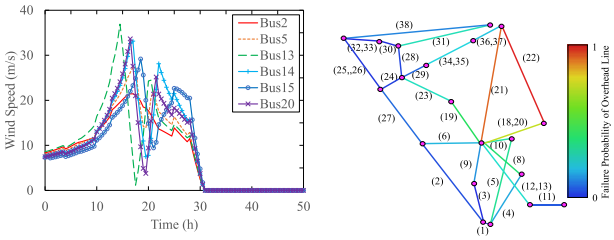

(a) wind speed (b) failure probability

Fig. 8. Wind speed at nodes and failure rate distribution of the line.

TABLE I
RESULTS OF THE OVERHEAD LINE PARTITION

Line	Units	Line	Units	Line	Units
(1, 2)	9	(8, 9)	138	(15, 24)	115
(1, 3)	177	(8, 10)	138	(16, 17)	57
(1, 5)	70	(11, 13)	106	(16, 19)	51
(2, 4)	106	(11, 14)	93	(17, 18)	32
(2 ,6)	160	(12, 13)	106	(17, 22)	234
(3, 9)	99	(12, 23)	215	(18, 21)	57
(4, 9)	86	(13, 23)	193	(19, 20)	88
(5, 10)	74	(14, 16)	86	(20, 23)	48
(6, 10)	51	(15, 16)	38	(21, 22)	151
(7, 8)	51	(15, 21)	109		

model into KKT conditions. The two-level problem is transformed into single-level mixed integer linear programming model which is solved by the commercial solver.

In the above model, equations (12), (16), (31), (34), (35) are an indicator function. For example, equation (12) can be linearized by introducing a penalty factor, that is, maximum value U_D and minimum value L_D of $D_{i,m-1}-aD_{i,0}$, as follows

$$L_D\left(1-Z_{i',m}\right) \le D_{i,m-1}-\alpha D_{i,0} \le U_D Z_{i',m}-\varepsilon \quad (41)$$

The equations (22), (24), (36), (37) involve variable multiplication, which can be linearized through Big M theory [37] or multiple inequality constraints.

V. CASE STUDIES

This paper uses the IEEERTS-79 system to study the impact of typhoons on the resilience of CPPS [38]. The geographic location of the line and the structure of the communication network are shown in Fig. 7. The average distance between towers is 500 m. To better analyze the impact of typhoons on overhead lines, each line is divided by average line span which is 500m as a unit whose weather intensity and fault model are consistent. The division result is shown in Table I. The parameters of overhead lines including power lines and OPGW are set as: $V_{d,wire} = 20$ m/s, $a = 11$, $b = -18$. The initial load ratio of the line is 0.6.

The system communication mode is synchronous digital hierarchy (SDH) through optical fiber. Since electric power trunk communication network must firstly meet the demand of real-time performance and reliability design of information transmission required by power grid control services [39], bandwidth constraints are not considered. The propagation delay and network equipment delay are 5 μs/km and 25 μs respectively. The concrete calculation method is shown in [40]. The delay requirement of dispatching automation service is taken as 30ms [39].

Typhoon Maria in 2018 is taken as an example to verify the method effectiveness. The typhoon data come from the Joint Typhoon Warning Center (JTWC) [41]. The typhoon parameters at the middle moment between the two adjacent sets of data are determined by linear sampling. We take 2018-7-10 12:00 as the start simulation time. the initial coordinates of the typhoon are (120°E, 26.4°N). The red line in the Fig. 7 (a) is the trajectory of the typhoon center, and the dotted circle is the position of the maximum wind speed during the typhoon passes.

Normally, the line will be repaired after the typhoon passes. Assume that each maintenance team of the communication line and the power line has one group, that is, $R_{CL} = 1$ and $R_{PL} = 1$. The parameter settings of the overhead line are set as $T_{ij}^{CP} = 1h$, $T_{ij}^{LP} = 1h$. Information node failure at any terminal of the power line requires additional repair time $\Delta T_{L,ij} = 0.5h$. A line may fail in multiple segments, and the maintenance team will repair them one by one. Parameter settings of the generator is: $K_g = 0.5P_{g,max}/h$. $\Delta T_{G,g} = 0.5h$. The power-supply coefficient α is 0.7 and the simulation step is 0.5h, which is implemented on MATLAB 2016b by CPLEX 12.6.3 through the YALMIP toolbox.

Since all nodes except node 2 are within the maximum wind circle when the typhoon passes, the distribution of wind speeds is bimodal. Because node 13 is closer to the typhoon landing point, its maximum wind speed is significantly higher than that of node 14. However, although node 15 is farther from the coastline than node 5, the cyclone direction at this point and the wind moving direction are usually at an acute angle during the typhoon and the wind speed is higher. As the distance between the line and the coastline increases, the failure rate declines sharply. Although line 22 and line 19 are shorter than line 21 and line 27, the typhoon passes earlier and the failure rate is higher. Therefore, the protection of long-distance transmission lines along the coast should be emphasized.

A. Numerical Simulation of the Typhoon

The wind speed of some nodes and the predicted failure probability distribution for each line are shown in Fig. 8.

B. Resilience Analysis

The failure severity of the overhead line at each moment is shown in Fig. 9. It can be found that due to the geographical coupling of power lines and optical cables, the fault patterns

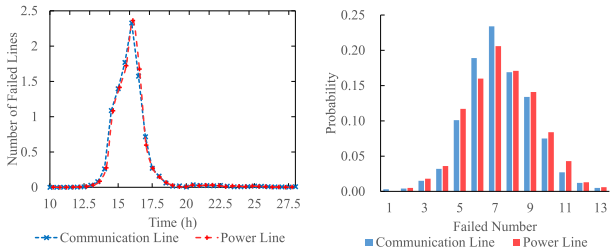

(a) time distribution (b) fault scale

Fig. 9. Severity of overhead line failures.

TABLE II
THE FAULT PARAMETERS IN THE SCENARIO

Time(h)	Power Line	OPGW	Time(h)	Power Line	OPGW
14.5	22(3 cuts)	8,22	17		37
15	5,21	5	17.5	24	29
15.5	18,21,22	11	18	33	
16	18,21		18.5	34	
16.5		9	19		

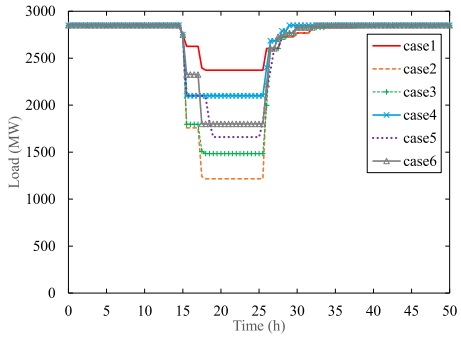

Fig. 10. The load curve of CPPS under different schemes.

are approximately the same. Most of the faults are concentrated in 13 h-19 h, and there is an approximately 80% probability of N-5 to N-9 failures. Therefore, we take N-7 failures as a typical scenario to analyze and compare the impact of different improvement measures on system resilience. The start time of maintenance is set to 25 h. The maximum wind speed in the area is only 11 m/s at this time and the failure probability is extremely small. The specific fault units in the scenario are shown in Table II. The load curves of different cases are shown in Fig. 10.

Case 1: The resilience is quantified by using the evaluation framework in [9] from the perspective of weather intensity and power infrastructure performance. The information system is assumed to work normally during the failure period.

Case 2: Based on Case 1, assessment process takes the proposed cyber-physical coupling into account, and the line and the generator are restored manually.

Case 3: Based on Case 2, the OPF and cyber-physical collaborative recovery consider the information network constraints.

Case 4: Based on Case 3, the line is reinforced and its design wind speed is increased from 22 m/s to 23.5 m/s. During the typhoon, the average number of failures of communication lines is reduced to 3, and the average number of power lines failures is reduced to 4. Assume that there is no fault in power lines 23, 33, 34 or in communication lines 5, 9, 11 and 37 in this scenario.

Case 5: Based on Case 3, the power communication adopts a buried optical cable. The communication line maintains normal operation during the typhoon.

Case 6: Based on Case 3, the communication substation is equipped with UPS and the power-supply coefficient is reduced from 0.7 to 0.3.

Case 1 does not consider the interactions between the physical power system and the control system. Its simulated fault scale is significantly smaller than other methods. Because of the control system malfunction, the load loss in Case 2 is 24621.8MWh more than that in Case 1. It can be seen that modeling and evaluating the physical layer only and ignoring the information layer may result in the large deviation in assessment results in cyber-physical integrated conditions.

Case 3 runs OPF considering the information network constraints. By reducing the load on nodes 4, 6 and 10, the power supply for nodes 3 and 5 is ensured. When failures happen on information nodes 4 and 6, generators on nodes 1, 2 can work normally which reduces the outage scale. In this scenario, the unobservable nodes are 4, 6, 7, 8, 13, 14. Only the fault lines 5, 18 and 22 need manual assistance. Because of slighter accident and reasonable repair sequence, Case 3 recovers faster than Case 2.

In Case 4, lines 23 and 34 play a key supporting role in power transmission from power generation area 16, 18, 21, 22 to the middle load area. Their normal operation has increased the output power of these generators by 257.5MW. The normal operation of communication line 11 enable the generation node 7 to respond to power flow adjustment. The result shows that the reduction of the failure scale can improve the power-supply level.

In Case 5, all communication lines can work normally. Buried communication line 11 makes the generator node 7 under control during the disaster and response to emergency. Simulation shows that this strategy reduces the risk of communication interruption during the typhoon.

In Case 6, after the failure of power lines 22 and 21, the transmission channels between generation nodes 13 is cut off. The interruption of line 5 reduces the maximum transmission capacity by 43.79% from generation node 2 to load nodes 6, 9, and 10. Generation node 13 will bear part of their load, which reduces the load of this node to 0.64 of the initial value, which is lower than α the information node requires and the generator will be out of control. Since the supply-level for node 13 is greater than α, this node can maintain normal operation.

In Table III, each index is the average value of 1000 simulation results in different schemes. There is a negative relationship between communication line failures, information node failures and system resilience, which shows that the information system contributes to the propagation of power failures. Although the scale of power line faults in Case 5 is almost two times that of Case 4, the load loss increment is smaller, indicating that generator cutoff is an important factor in load reduction. The circulation of communication channels between generators and the control center can reduce the load reduction level. Case 6 is significantly higher than Case 4 and

TABLE III
COMPARISON OF FAILURE SCALES IN DIFFERENT CASES

Index (mean value)	Case 1	Case 2	Case 3	Case 4	Case 5	Case 6
Line Fault Scale	7.326	7.332	7.321	3.667	7.323	7.332
Link Fault Scale	0	6.654	6.636	3.283	0	6.646
Load Loss (MWh)	9998	33801	28922	9891	12254	22079
Failure Rate of Info Nodes	0	0.4604	0.4438	0.1489	0.1403	0.1979
Maintenance Time(h)	11.221	14.212	14.355	6.413	13.133	13.575
Resilience	0.9064	0.6833	0.7303	0.9065	0.8857	0.7936

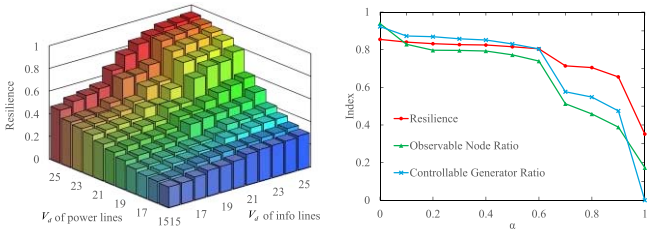

(a) impacts of reinforcement (b) impacts of α

Fig. 11. The resilience under reinforcement schemes and different α.

Case 5 in terms of the scale of link faults and load loss, but the difference in the failure rate of communication nodes is relatively small, indicating that the power-supply coefficient has a greater impact on the operation of information nodes than the interruption of communication lines.

C. Research on Resilience Improvement Measures

According to the definition, there are three ways to improve system resilience: reduce the incidence of system failures, reduce the impact of failures on system operation, and increase system repair efficiency. Therefore, this paper studies the impact of different enhancement measures on CPPS resilience from these three dimensions.

1) System Design: Reducing the failure frequency can be achieved by strengthening system components, optimizing design standards of disaster prevention, and improving system robustness. The integration of information systems has increased the failure types and propagation modes. Here we study the impact of the reinforcement of power lines and communication lines on system resilience. The simulation results are shown in Fig. 11 (a).

From the figure it can be found that strengthening the power line will improve the system's resilience more significantly. This is because communication line failure will not directly lead to load reduction. The generator can continue running through the governor without communication when the power grid remains the structure. However, the power line interruption will not only cause load reduction resulting in the communication node with insufficient power-supply but also give rise to runaway generator tripping. Therefore, power lines have a greater impact on resilience. It is recommended to prioritize power line reinforcement in a resource-constrained environment.

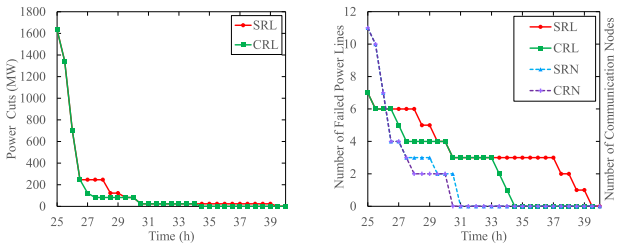

(a) load loss (b) faults number

Fig. 12. The influence of information system on failure recovery.

2) Response Capability: The response capability reflects the system's absorbing and adapting ability to disturbances. After a power failure, emergency plans are adopted to regulate the power flow distribution and enable the standby generator to maintain the power-supply level. The execution of these instructions relies on the information system. Fig. 11 (b) reflects the influence of the power-supply coefficient on system resilience.

The decrease in α reduces the dependence of the information system on the power system. With α dropping, the number of observable nodes increases significantly and expands the control area, which improves the response margin and reduces the load reduction. The three curves are positively correlated. Considering that information transfer is more flexible, generator control will be affected only when the number of unobservable nodes reaches a certain amount.

3) Collaborative Recovery: The failure of information equipment prevents the maintenance crew from obtaining relevant fault information in time. The reduction in the system automation level increases the repair time. Take the Case2 in Section V-B as an example to study the supporting effects of the information system in power system restoration. The results is shown in Fig. 12.

Compared to the one that does not consider the assistance of the communication device, the curves of collaborative recovery for lines (CRL) and collaborative recovery for nodes (CRN) compared with separate recovery ones (SRL, SRN) show that collaborative repair takes into account the mutual influence between power nodes and information nodes during the recovery process, and the repair efficiency is improved. Fault power lines 18, 22 reduce the extra artificial restoration time for one end and 5 speeds up recovery from the both ends. The rest lines reduce all extra repair time. Because of the redundancy of the transmission line capacity, the load is restored before the power line recovery, and the number of unobservable nodes decreases earlier than that of failed power lines. The restoration of information nodes will promote the subsequent repair of power lines. According to this characteristic, the recovery efficiency of power failure can be significantly improved.

VI. CONCLUSION

This paper proposes a CPPS resilience assessment method considering cyber-physical interactions. Based on the actual typhoon data, five different schemes are designed according

to the actual prevention measures to verify the feasibility of the proposed method. The simulation results show that the increased coupling between the information system and the power system will expand the scale of power failures and the failure rate of communication nodes, but the normal operation of the information system can have a positive effect on the emergency response and failure recovery of the power system. On this basis, the impact of enhancement measures on CPPS resilience is analyzed. According to the characteristics of typhoon disasters, system structure and source-load distribution, reinforcement for key lines and cyber-physical decoupling for some important components will effectively improve the system's resistance to extreme weather conditions.

However, it is important to point out that this paper simplifies the operation model of information systems and power systems. The influence of communication delay, node voltage, system frequency and other factors on the fault propagation and recovery of CPPS under extreme weather conditions will be considered in future work.

REFERENCES

[1] M. Farzaneh and K. Savadjiev, "Statistical analysis of field data for precipitation icing accretion on overhead power lines," *IEEE Trans. Power Del.*, vol. 20, no. 2, pp. 1080–1087, Apr. 2005.

[2] Y. Cai and M. W. Golay, "A framework analyzing system status and human activities: Illustrated using 2011 Fukushima nuclear power plant accident scenarios," *Nucl. Eng. Design*, vol. 373, Mar. 2021, Art. no. 111025.

[3] S. Xin, Q. Guo, H. Sun, B. Zhang, J. Wang, and C. Chen, "Cyber-physical modeling and cyber-contingency assessment of hierarchical control systems," *IEEE Trans. Smart Grid.*, vol. 6, no. 5, pp. 2375–2385, Sep. 2015.

[4] D. Meyer, "Overview of recommendations by U.S.–Canada task force to prevent or minimize scope of future blackouts," in *Proc. IEEE Power Energy Soc. Gen. Meeting (PESGM)*, Denver, CO, USA, 2004, p. 579.

[5] J. Lu, M. Zeng, X. Zeng, Z. Fang, and J. Yuan, "Analysis of ice-covering characteristics of China Hunan power grid," *IEEE Trans. Ind. Appl.*, vol. 51, no. 3, pp. 1997–2002, May/Jun. 2015

[6] Y. Wang, C. Chen, J. Wang, and R. Baldick, "Research on resilience of power systems under natural disasters—A review," *IEEE Trans. Power Syst.*, vol. 31, no. 2, pp. 1604–1613, Mar. 2016.

[7] M. Bruneau and A. Reinhorn, "Exploring the concept of seismic resilience for acute care facilities," *Earthquake Spectra*, vol. 23, no. 1, pp. 41–62, Feb. 2007.

[8] M. Panteli, P. Mancarella, D. N. Trakas, E. Kyriakides, and N. D. Hatziargyriou, "Metrics and quantification of operational and infrastructure resilience in power systems," *IEEE Trans. Power Syst.*, vol. 32, no. 6, pp. 4732–4742, Nov. 2017.

[9] Y. Yang, W. Tang, Y. Liu, Y. Xin, and Q. Wu, "Quantitative resilience assessment for power transmission systems under typhoon weather," *IEEE Access*, vol. 6, pp. 40747–40756, 2018.

[10] X. Liu *et al.*, "A planning-oriented resilience assessment framework for transmission systems under typhoon disasters," *IEEE Trans. Smart Grid*, vol. 11, no. 6, pp. 5431–5441, Nov. 2020.

[11] S. Ma, B. Chen, and Z. Wang, "Resilience enhancement strategy for distribution systems under extreme weather events," *IEEE Trans. Smart Grid*, vol. 9, no. 2, pp. 1442–1451, Mar. 2018.

[12] M. Panteli, D. N. Trakas, P. Mancarella, and N. D. Hatziargyriou, "Boosting the power grid resilience to extreme weather events using defensive islanding," *IEEE Trans. Smart Grid*, vol. 7, no. 6, pp. 2913–2922, Nov. 2016.

[13] H. Sekhavatmanesh and R. Cherkaoui, "A novel decomposition solution approach for the restoration problem in distribution networks," *IEEE Trans. Power Syst.*, vol. 35, no. 5, pp. 3810–3824, Sep. 2020.

[14] Z. Lin, F. Wen, and Y. Xue, "A restorative self-healing algorithm for transmission systems based on complex network theory," *IEEE Trans. Smart Grid*, vol. 7, no. 4, pp. 2154–2162, Jul. 2016.

[15] R. Sun, Y. Liu, and L. Wang, "An online generator start-up algorithm for transmission system self-healing based on MCTS and sparse autoencoder," *IEEE Trans. Power Syst.*, vol. 34, no. 3, pp. 2061–2070, May 2019.

[16] A. Clark and S. Zonouz, "Cyber-physical resilience: Definition and assessment metric," *IEEE Trans. Smart Grid*, vol. 10, no. 2, pp. 1671–1684, Mar. 2019.

[17] Tushar, V. Venkataramanan, A. Srivastava, and A. Hahn, "CP-TRAM: Cyber-physical transmission resiliency assessment metric," *IEEE Trans. Smart Grid*, vol. 11, no. 6, pp. 5114–5123, Nov. 2020.

[18] V. Venkataramanan, A. Hahn, and A. Srivastava, "CP-SAM: Cyber-physical security assessment metric for monitoring microgrid resiliency," *IEEE Trans. Smart Grid*, vol. 11, no. 2, pp. 1055–1065, Mar. 2020.

[19] L. Guo, J. Shu, X. Luo, and H. Sun, "EMS communication routings' optimisation to enhance power system security considering cyber-physical interdependence," *IET Cyber-Phys. Syst.Theor. Appl.*, vol. 1, no. 3, pp. 44–53, Mar. 2008.

[20] L. Xu, Q. Guo, T. Yang, and H. Sun, "Robust routing optimization for smart grids considering cyber-physical interdependence," *IEEE Trans. Smart Grid*, vol. 10, no. 5, pp. 5620–5629, Sep. 2019.

[21] G. Huang, J. Wang, C. Chen, and C. Guo, "Cyber-constrained optimal power flow model for smart grid resilience enhancement," *IEEE Trans. Smart Grid*, vol. 10, no. 5, pp. 5547–5555, Sep. 2019.

[22] Z. Liu and L. Wang, "Leveraging network topology optimization to strengthen power grid resilience against cyber-physical attacks," *IEEE Trans. Smart Grid*, vol. 12, no. 2, pp. 1552–1564, Mar. 2021.

[23] R. Sun and Y. Liu, "An on-line generator start-up strategy based on deep learning and tree search," in *Proc. IEEE Power Energy Soc. Gen. Meeting (PESGM)*, Portland, OR, USA, 2018, pp. 1–5.

[24] R. Rocchetta, E. Zio, and E. Patelli, "A power-flow emulator approach for resilience assessment of repairable power grids subject to weather-induced failures and data deficiency," *Appl. Energy*, vol. 210, pp. 339–350, Jan. 2018.

[25] M. Miyazaki, T. Ueno, and S. Unoki, "Theoretical investigations of typhoon surges along the Japanese coast (II)," *Oceanogr. Mag.*, vol. 12, no. 2, pp. 103–118, 1962.

[26] M. E. Batts, M. R. Cordes, L. R. Russell, J. R. Shaver, and E. Simiu, "Hurricane wind speeds in the United States," *J. Struct. Div.*, vol. 106, no. 10, pp. 2001–2016, Oct. 1980.

[27] F. Xiao, J. D. McCalley, Y. Ou, J. Adams, and S. Myers, "Contingency probability estimation using weather and geographical data for on-line security assessment," in *Proc. Int. Conf. Probab. Methods Appl. Power Syst.(PMAPS)*, Stockholm, Sweden, 2006, pp. 1–7.

[28] V. Rosato, L. Issacharoff, F. Tiriticco, S. Meloni, S. D. Porcellinis, and R. Setola, "Modelling interdependent infrastructures using interacting dynamical models," *Int. J. Crit. Infrastruct.*, vol. 4, nos. 1–2, pp. 63–79, 2008.

[29] S. Azizi, M. Sun, G. Liu, M. Popov, and V. Terzija, "High-speed distance relaying of the entire length of transmission lines without signaling," *IEEE Trans. Power Deliv.*, vol. 35, no. 4, pp. 1949–1959, Aug. 2020.

[30] E. Litvinov, S. Zhang, X. Luo, and T. Zheng, "Synchrophasor-based emergency generation control for area balancing," *IEEE Trans. Smart Grid*, vol. 10, no. 5, pp. 5831–5840, Sep. 2019.

[31] Z. Li, M. Shahidehpour, and F. Aminifar, "Cybersecurity in distributed power systems," *Proc. IEEE*, vol. 105, no. 7, pp. 1367–1388, Jul. 2017, doi: 10.1109/JPROC.2017.2687865.

[32] S. Zhang, W. Ma, M. Yu, F. Zhang, and J. Chen, "Design of monitoring system for redundant communication power supply based on ZigBee," *J. Phys. Conf. Series*, vol. 1754, no. 1, pp. 12046–12052, Feb. 2021.

[33] Z. Bie, Y. Lin, G. Li, and F. Li, "Battling the extreme: A study on the power system resilience," *Proc. IEEE*, vol. 105, no. 7, pp. 1253–1266, Jul. 2017.

[34] Z. Y. Chen and X. F. Wang, "A congestion awareness routing strategy for scale-free networks with tunable clustering," *Phys. A, Stat. Mech. Appl.*, vol. 364, pp. 595–602, May 2006.

[35] H. Bevrani and T. Hiyama, "On load–frequency regulation with time delays: Design and real-time implementation," *IEEE Trans. Energy Convers.*, vol. 24, no. 1, pp. 292–300, Mar. 2009.

[36] H. Banakar, N. Alguacil, and F. D. Galiana, "Electrothermal coordination part I: theory and implementation schemes," *IEEE Trans. Power Syst.*, vol. 20, no. 2, pp. 798–805, May 2005.

[37] T. Ding, C. Li, C. Yan, F. Li, and Z. Bie, "A bilevel optimization model for risk assessment and contingency ranking in transmission system reliability evaluation," *IEEE Trans. Power Syst.*, vol. 32, no. 5, pp. 3803–3813, Sep. 2017.

[38] P. M. Subcommittee, "IEEE reliability test system," *IEEE Trans. Power App. Syst.*, vol. PAS-98, no. 6, pp. 2047–2054, Nov. 1979.

[39] L. Jie, L. Gang, and M. Xin, "Analysis of power grid control service information and communication network reliability model," in *Proc. 2nd Int. Conf. Model. Simulat. Visualization Methods*, Sanya, China, 2010, pp. 233–238.
[40] S. Huang, S. Rai, and B. Mukherjee, "Survivable differential delay aware multi-service over SONET/SDH networks with virtual concatenation," in *Proc. Conf. Opt. Fiber Commun. Nat. Fiber Opt. Eng. Conf.*, Anaheim, CA, USA, 2007, pp. 1–3.
[41] Joint Typhoon Warning Center. *Western North Pacific Ocean Best Track Data*. Accessed: Mar. 10, 2021. [Online]. Available: http://www.metoc.navy.mil/jtwc

Baozhong Ti received the bachelor's degree from North China Electric Power University, Beijing, China, in 2016, where he is currently pursuing the Ph.D. degree under the direction of Prof. G. Li. His research is mainly focused on reliability assessment and failure recovery of cyber-physical power system.

Gengyin Li (Member, IEEE) received the B.S., M.S., and Ph.D. degrees in electrical engineering from North China Electricity Power University in 1984, 1987, and 1996, respectively. Since 1987, he has been with the School of Electrical and Electronic Engineering, North China Electric Power University, where he is currently a Professor. His research interests include HVDC transmission, analysis and control of power system with renewable energy, and power system economics.

Ming Zhou (Senior Member, IEEE) received the B.S., M.S., and Ph.D. degrees in electrical engineering from North China Electric Power University in 1989, 1992, and 2006, respectively. Since 1992, she has been with the School of Electrical and Electronic Engineering, North China Electric Power University, where she is currently a Professor. Her research interests include power system analysis and reliability, power system economics, HVDC transmission, electricity market, and power quality analysis.

Jianxiao Wang (Member, IEEE) received the double bachelor's degrees in electrical engineering and economic management and the Ph.D. degree from the Department of Electrical Engineering, Tsinghua University, Beijing, China, in 2014 and 2019, respectively. He is currently an Assistant Professor with the Department of Electrical and Electronic Engineering, North China Electricity Power University, Beijing. His research interests include cyber-physical system, energy integration planning, market mechanism design, energy economics, and policy. He was awarded as the Outstanding Ph.D. Graduate of Tsinghua University, and Junior Fellowships for Advanced Innovation Think-Tank Programming by China Association for Science and Technology.